J Mol Model (2008) 14:1065–1070
DOI 10.1007/s00894-008-0339-3

ORIGINAL PAPER

DFT-based theoretical QSPR models of *Q-e* parameters for the prediction of reactivity in free-radical copolymerizations

Xinliang Yu · Wanqiang Liu · Fang Liu · Xueye Wang

Received: 9 April 2008 / Accepted: 13 June 2008 / Published online: 24 July 2008

Abstract Density functional theory (DFT) calculations at the B3LYP/6–31G(d) level were carried out for 47 vinyl monomers with structures $C^1H_2 = C^2HR^3$, and the calculated quantum chemical descriptors were used to construct quantitative structure–property relationship (QSPR) models of the reactivity parameters of monomers *Q* and *e*. Stepwise multiple linear regression analysis (MLRA) and artificial neural networks (ANN) were adopted to generate the models. Simulated with the final optimum back-propagation (BP) neural networks, the results show that predicted ln*Q* and *e* values are in good agreement with experimental data, with test sets possessing correlation coefficients of 0.982 for lnQ and 0.943 for *e*. The proposed ANN models have better prediction ability than existing models.

Keywords Artificial neural network · Density functional theory · Monomers · QSPR · Quantum chemical descriptors · Reactivity parameters of monomers (*Q*,*e*)

X. Yu (✉) · F. Liu
Department of Chemistry and Chemical Engineering,
Hunan Institute of Engineering,
Xiangtan, Hunan 411104, China
e-mail: yxl@hnie.edu.cn

W. Liu
School of Chemistry and Chemical Engineering,
Hunan University of Science and Technology,
Xiangtan, Hunan 411201, China

X. Wang
College of Chemistry, Xiangtan University,
Xiangtan, Hunan 411105, China

Introduction

The *Q–e* scheme may be regarded as an empirical method for establishing quantitative relationships for monomer activity in copolymerizations. It has been proposed that the rate constant for a radical–monomer reaction, for example, for the reaction of radical M_1 with monomer M_2, be written as: $k_{12} = P_1 Q_2 \exp(-e_1 e_2)$, where P_1 and Q_2 are measures of the resonance stabilization of M_1 and M_2, respectively, and e_1 and e_2 are measures of their respective polarities. Assuming that the reactivity of a growing polymeric radical depends only on the nature of the terminal radical unit, similar equations for the basic propagation rate constants k_{11}, k_{21}, and k_{22} can be derived: $k_{11} = P_1 Q_1 \exp(-e_1 e_1)$, $k_{21} = P_2 Q_1 \exp(-e_2 e_1)$, $k_{22} = P_2 Q_2 \exp(-e_2 e_2)$. The reactivity ratios, $r_1 = k_{11}/k_{12}$ and $r_2 = k_{22}/k_{21}$, can be used to eliminate the parameter *P* for the free radical M_1 [1]:

$$r_1 = \frac{Q_1}{Q_2} \exp[-e_1(e_1 - e_2)] \quad (1)$$

$$r_2 = \frac{Q_2}{Q_1} \exp[-e_2(e_2 - e_1)] \quad (2)$$

Hence, the reactivity ratios r_1 and r_2 depend only on the parameters *Q* and *e*. In practice, the *Q–e* scheme defines a reference monomer to which all other monomers can be related. The most popularly used reference is styrene (*Q*= 1.0 and *e*=− 0.8) [2, 3]. The *Q* and *e* values of any other monomer can be determined by using Eqs. 1 or 2 based on the experimental reactivity ratios and the *Q* and *e* values of the reference monomer. Equation 1 (or 2) may be arranged as a logarithmic form, which provides a more convenient linear solution:

$$\left\{[\ln(Q_1/r_1)] - e_1^2\right\} = -e_1 e_2 + \ln Q_2 \quad (3)$$

Despite its shortcomings, the *Q–e* scheme has proven to be remarkably useful, and continues to be essentially the only general reactivity scheme for predicting radical copolymerizations in use today [4, 5]. The *Q–e* scheme, which is based on a large database of kinetic rate constants, can be used for predicting the relative reactivity in free-radical copolymerizations without recourse to experimental determination of additional kinetic rate constants. But the standard scheme is limited because of the shortage of *Q* and *e* parameter values, which are difficult to obtain experimentally [6, 7]. Therefore, the development of reliable quantitative structure–property relationship (QSPR) models for prediction of basic *Q* and *e* parameters is of real interest, particularly in the case of new monomers for which experimental investigation would be expensive [4, 8]. The concept of QSPR is to transform searches for compounds with desired properties using chemical intuition and experience into a mathematically quantified and computerized form. Once a satisfactory correlation between structure and property is found, any number of compounds, including those not yet synthesized, can be readily screened by computer in order to select chemical structures with the desired properties. Thus, the QSPR approach conserves resources and accelerates the process of development of new molecules for any purpose [9].

To our knowledge, few studies of QSPRs for parameters *Q* and *e* have been published in recent years [4, 8]. Zhan et al. have constructed QSPR models for parameters ln*Q* and *e* with calculated electronegativities and reaction free energies; however, these models have not been validated with test sets [4]. In addition, Toropov et al. have performed QSPR test analysis by optimizing the correlation weights of the local invariants of molecular graphs representing monomer structures in order to construct models of *Q* and *e*. Test sets have correlation coefficients of 0.823 for *Q* and 0.895 for *e* [8]. Although the correlation coefficients are low, the models have statistical significance.

In principle, quantum chemical theory can provide precise quantitative descriptors of molecular structures and their chemical properties. Furthermore, quantum chemical descriptors have clear physical meanings [9, 10, 11]. The goal of this paper is to produce robust QSPR models that can predict the reactivity parameters *Q* and *e* values of 47 vinyl monomers with structures $C^1H_2 = C^2HR^3$. The quantum chemical descriptors calculated using density functional theory (DFT) methods were correlated with experimental ln*Q* and *e* values using nonlinear artificial neural network (ANN) methods.

Materials and methods

Table 1 shows the data sets for 47 reactivity parameters of vinyl monomers (taken from [12]). The entire set contains a wide range of reactivity parameters of monomers (*Q*, *e*) values, and is characterized by a high degree of structural variety, for example, the functionalities present in the side chains include halides, ketones, acids, sulfides, esters, ethers, and aromatic rings.

All monomers were fully optimized and calculated by DFT [13, 14] using the program GAUSSIAN 03 [15] at the B3LYP [16] /6–31G(d) [17] level. The keywords were OPT, FREQ, POLAR and POP = REG. Some necessary quantum chemical descriptors were calculated. These descriptors included Mulliken and atomic polar tensor (APT) [18] charges of C^1, C^2 and R^3 ($q_{MC^1}, q_{MC^2}, q_{MC^3}, q_{AC^1}, q_{AC^2}, and\ q_{AR^3}$), the most positive net atomic charge on hydrogen atoms in a molecule (q^+), the net charge of the most negative atom (q^-), the total dipole moment (μ), the energy of the highest occupied molecular orbital (E_{HOMO}) and the energy of the lowest unoccupied molecular orbital (E_{LUMO}) [19, 20]. The descriptor R^3 expressed the atom connected to C^2 directly.

A few other descriptors were defined, such as ΔE_g [21], $\hat{q}_{AC^1,R^3}, \overline{q}_{MC^1,R^3}, R_{MC^1/R^3}, q_{MC^1}, R_{MR^3/AC^1}$, and $R_{E_{LUMO/\alpha}}$. The detailed descriptors are presented in Table 2.The average polarizability of molecules (α) was defined as follows:

$$\alpha = (\alpha xx + \alpha yy + \alpha zz)/3 \tag{4}$$

where α_{xx}, α_{yy} and α_{zz} are exact polarizability in the *x*-, *y*-, and *z*-coordinates, respectively. α increases with the size of the species either as a result of an increase with the number of electrons or by the expansion of the molecular radius. The difference of APT charges between C^1 and R^3, $\hat{q}_{AC^1,R^3}$, was calculated with following equation:

$$\hat{q}_{AC^i,R^3} = q_{AC^i} - q_{AR^3} \tag{5}$$

The average Mulliken atomic charges of C^1 and R^3 ($\overline{q}_{MC^1,R^3}$) was defined as follows:

$$\overline{q}_{MC^1,R^3} = \frac{q_{MC^{1i}} \times q_{MR^3}}{q_{MC^1} + q_{MR^3}} \tag{6}$$

The ratio between Mulliken charges of atoms C^1 and R^3 was given by Eq. 7:

$$R_{MC^1/R^3} = \frac{q_{MC^1}}{q_{MR^3}} \tag{7}$$

Similar equations for descriptors $R_{MR3/AC1}$ and $R_{E_{LUMO/\alpha}}$ can be derived. In this paper, the 18 descriptors stated above were calculated to fit parameters ln*Q* and *e*.

Stepwise multiple linear regression analysis (MLRA) was used for 47 reactivity parameters *Q* and *e* (in Table 1) respectively, in order to select the respective best subsets of descriptors from the 18 descriptors mentioned above. Subset size was increased until addition of another descriptor did not significantly improve the standard error of the estimate. Furthermore, a variance inflation factor (VIF) was calculated to see if multi-colinearities existed between the descriptors in a model. Models were not accepted if they contained

Table 1 Monomers used in this study with observed and calculated ln$Q$ and e values

No.	Monomer	Modeling ln$Q$			Modeling e		
		Experimental ln$Q$	Calculated ln$Q$	Δln$Q$ [a]	Experimental e	Calculated e	Δe [b]
	Training set						
1	Vinyl acetate	-3.6497	-3.4066	-0.2431	-0.88	-0.789	-0.091
2	Vinyl bromide	-3.2702	-2.9447	-0.3255	-0.23	-0.290	0.060
3	Vinyl butyrate	-3.7297	-3.4476	-0.2821	-0.89	-0.797	-0.094
4	Vinyl benzoate	-3.5066	-2.472	-1.0346	-0.89	-1.187	0.297
5	Vinyl butyl ether	-3.2702	-3.6836	0.4134	-1.5	-1.808	0.308
6	Vinyl chloride	-2.8824	-3.1623	0.2799	0.16	0.116	0.044
7	Vinyl chloroacetate	-3.2442	-2.8622	-0.3820	-1.61	-1.321	-0.289
8	Vinyl cinnamate	-1.7148	-1.9432	0.2284	0.76	0.757	0.003
9	Vinyl dodecyl ether	-3.1942	-3.6966	0.5024	-1.69	-1.864	0.174
10	Vinyl ethyl ether	-4.0174	-3.6613	-0.3561	-1.8	-1.731	-0.069
11	Vinyl ethyl sulfide	-1.3093	-1.6975	0.3882	-1.31	-1.217	-0.093
12	Vinyl fluoride	-4.8283	-3.8794	-0.9489	0.72	0.703	0.018
13	Vinyl hendecanoate	-2.8824	-3.4725	0.5901	-0.84	-0.737	-0.103
14	Vinyl isobutyl sulfide	-0.7133	-1.7084	0.9951	-0.95	-1.179	0.229
15	Vinyl laurate	-4.5099	-3.4642	-1.0457	-0.54	-0.748	0.208
16	Vinyl methyl sulfide	-0.8675	-1.6292	0.7617	-1.66	-1.670	0.010
17	Vinyl octadecyl ether	-3.7297	-3.9081	0.1784	-1.93	-1.873	-0.057
18	Vinyl pelargonate	-3.0791	-3.4701	0.3910	-1.22	-0.745	-0.475
19	Vinyl phenyl ketone	0.1484	0.1377	0.0107	1.02	1.091	-0.071
20	Vinyl propionate	-3.6119	-3.3877	-0.2242	-0.68	-0.789	0.109
21	Vinyl tert-butyl sulfide	-3.0791	-1.8673	-1.2118	-2.2	-1.735	-0.465
22	Vinyl 4-chlorocyclohexyl ketone	-0.4155	-0.158	-0.2575	-0.82	-0.779	-0.041
23	*p*-Vinylbenzylethylcarbinol	-0.3711	0.1952	-0.5663	-0.98	-0.708	-0.272
24	*p*-Vinylanthracene	-1.9661	-1.9739	0.0078	0.82	1.027	-0.207
25	*p*-Vinylbenzoic acid	1.6429	0.8542	0.7887	1.08	1.135	-0.055
26	Vinyl isocyanate	-1.9661	-3.1194	1.1533	-0.95	-1.133	0.183
27	Styrene	0.0000	0.0402	-0.0402	-0.8	-0.784	-0.016
28	Styrene, 2,5-dichloro-	0.4055	-0.0889	0.4944	0.94	0.252	0.688
29	Styrene, *m*-chloro-	0.9002	0.257	0.6432	-0.9	-0.387	-0.513
30	Styrene, *m*-nitro-	0.9783	1.1787	-0.2004	1.57	1.458	0.112
31	Styrene, *p*-chloro-	0.2852	0.2933	-0.0081	-0.64	-0.453	-0.187
32	Styrene, *p*-cyano-	1.0750	1.014	0.0610	-0.38	-0.394	0.014
33	Styrene, *p*-methyl-	0.0953	0.0865	0.0088	-0.63	-0.771	0.141
34	Styrene, *p*-l-(2-hydroxypropyl)-	0.0770	0.1615	-0.0845	-0.35	-0.499	0.149
35	Styrene, pentachloro-	-1.6094	-0.6813	-0.9281	0.79	0.992	-0.202
	Test set						
36	Vinyl dichloroacetate	-2.8302	-2.7964	-0.0338	-1.38	-1.310	-0.070
37	Vinyl ether	-3.5405	-3.2498	-0.2907	-1.16	-1.212	0.052
38	Vinyl formate	-3.1466	-3.5547	0.4081	-1.19	-1.177	-0.013
39	Vinyl methyl sulfoxide	-0.5108	-0.3014	-0.2094	-1.79	-1.933	0.143
40	Vinyl octyl ether	-3.9120	-3.6921	-0.2199	-1.57	-1.851	0.281
41	Vinyl stearate	-3.1466	-3.4726	0.3260	-0.97	-0.726	-0.244
42	Vinyl *N,N*-diethylcarbamate	-3.5756	-3.7491	0.1735	-1.1	-1.389	0.289
43	Styrene, 2,4,6-trimethyl-	-1.8971	-0.993	-0.9041	-0.58	-0.536	-0.044
44	Styrene, *m*-bromo-	0.2231	0.2979	-0.0748	-0.27	-0.316	0.046
45	Styrene, *p*-bromo-	0.2624	0.412	-0.1496	-0.68	-0.328	-0.352
46	Styrene, *p*-1-(2-hydroxybutyl)-	-0.3567	0.1848	-0.5415	-0.97	-0.712	-0.258
47	Styrene, *p*-2-(2-hydroxypropyl)-	0.1398	0.1513	-0.0115	-0.49	-0.529	0.039

[a] $\Delta\ln Q = \ln Q(\text{exp}) - \ln Q(\text{calc})$
[b] $\Delta e = e(\text{exp}) - e(\text{calc})$

Table 2 Selected descriptors for models of ln$Q$ and e using stepwise multiple linear regression analysis (MLRA) method. *LUMO* Lowest unoccupied molecular orbital, *HOMO* highest occupied molecular orbital, *APT* atomic polar tensor

Number	Descriptor	Definition	Unit
1	ΔE_g	Energy gap between LUMO and HOMO	au
2	$\hat{q}_{AC^1,R^3}$	APT charges difference between C^1 and R^3	au
3	$\overline{q}_{MC^1,R^3}$	Average Mulliken atomic charges of atoms C^1 and R^3	au
4	R_{MC^1/R^3}	Ratio between Mulliken atomic charges of atoms C^1 and R^3	/
5	E_{LUMO}	Energy of LUMO	au
6	q_{MC^1}	Mulliken charges on C^1	au
7	q^-	Net charge of the most negative atom of the molecule	au
8	$R_{M R^3/AC^1}$	Ratio of Mulliken charges on R^3 to APT charges on C^1	/
9	$R_{E_{LUMO}/\alpha}$	Ratio of E_{LUMO} to the average polarizbility of molecules (α)	/

descriptors with VIFs over a value of 10. The smallest subset of descriptors that did not compromise the standard error of the estimate and VIF-test was identified as optimal.

The experimental data from the 47 reactivity parameters Q and e in Table 1 were then divided into a training set and test set. In order to develop the ANN models for ln$Q$ and e from the training sets, three-layer, fully connected, back-propagation (BP) neural networks were adopted [22–24]. For each model, the number of neurons of the input layer was equal to the number of molecular descriptors taken from stepwise MLRA. The output layer contained one neuron representing the calculated value. The number of neurons in the hidden layer was optimized by trial and error, with the permission error being 0.00001, the momentum being 0.6, and the sigmoid parameter being 0.9. The trained network was used to predict the values of the test set. The sum of root-mean-square (rms) errors of the training set and the test set was used to evaluate the accuracy of each model. The rms error was defined as:

$$rms = \sqrt{\frac{\sum (f_i - x_i)^2}{N}} \tag{8}$$

where f_i is the predicted value for the ith compound, x_i is the observed value for the ith compound, and N represents the total number of compounds in the data set. The number of ANN hidden layer neurons was increased sequentially until no improvement was seen for that model.

Results and discussion

By carrying out the correlation between the 18 descriptors and 47 reactivity parameters Q and e with stepwise MLRA, two optimal MLRA models were obtained. The best subset of descriptors in the model of ln$Q$ comprises ΔE_g, $\hat{q}_{AC^1,R^3}$, $\overline{q}_{MC^1,R^3}$ and R_{MC^1/R^3}; while the best subset of descriptors in the model of e consists of E_{LUMO}, q_{MC^1}, q^-, $R_{M R^3/AC^1}$ and $R_{E_{LUMO}/\alpha}$. All these descriptors are shown in Table 2. The characteristics of the descriptors in each model are shown in Table 3.

Each best subset of descriptors selected from the stepwise MLRA method was then fed into an ANN as an input vector. The optimal conditions for the neural networks were obtained by adjusting parameters by trial-and-error. The architectures of the final optimum BP ANN are 4–1–1 for ln$Q$ and 5–2–1 for e. The calculated results from ANN methods of ln$Q$ and e are listed in Table 1 and depicted in Figs. 1 and 2, respectively, and indicate that all the experimental ln$Q$ and e values are close to predicted

Table 3 Characteristics of descriptors used in the MLRA models for ln$Q$ and e. *VIF* Variance inflation factor

Model	Descriptor	Coefficient	Standard error	Significance test	t - test	VIF
ln$Q$	Constant	5.127	0.820	0.000	6.250	/
	ΔE_g	-30.133	3.936	0.000	-7.657	1.951
	$\hat{q}_{AC^1,R^3}$	-1.673	0.241	0.000	-6.953	1.675
	$\overline{q}_{MC^1,R^3}$	0.575	0.197	0.006	2.924	1.074
	R_{MC^1/R^3}	-0.006	0.001	0.000	-4.914	1.196
e	Constant	0.818	0.509	0.116	1.607	/
	E_{LUMO}	-33.029	4.952	0.000	-6.669	5.279
	q_{MC^1}	1.802	0.734	0.018	2.456	1.135
	q^-	2.580	0.830	0.003	3.110	1.043
	$R_{M R^3/AC^1}$	-0.041	0.020	0.045	-2.069	1.026
	$R_{E_{LUMO}/\alpha}$	1,812.847	400.340	0.000	4.528	5.056

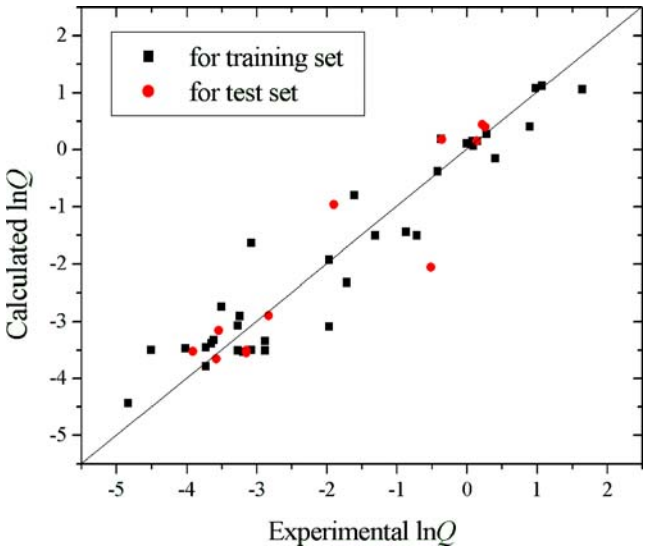

Fig. 1 Plot of calculated versus experimental ln$Q$ values

values. The training sets rms errors are 0.581 (R=0.949) for ln$Q$ and 0.234 (R=0.970) for e. The prediction sets rms errors are 0.367 (R=0.982) for ln$Q$ and 0.192 (R=0.943) for e, demonstrating the ability of the ANN models to generalize [4, 8]. Thus, the nonlinearity of ANN is useful for predicting reactivity parameters ln$Q$ and e, and the ANN models obtained in this paper are accurate.

The descriptors in the optimum MLRA models of ln$Q$ and e are all significant (see Table 3). According to statistical theory, when a VIF value in a model is greater than a certain limit (e.g., 10), the descriptor j is strongly correlated with the others and is not significant in explaining that model, and is thus unreliable. All the VIF values in this paper are less than 10 (see Table 3), which show that multi-colinearities do not exist between the descriptors in each model.

For the optimum model of ln$Q$ (see Table 3), the most significant descriptor is the energy gap between LUMO and HOMO, ΔE_g. According to the frontier molecular orbital (FMO) theory of chemical reactivity [19, 20], the highest occupied molecular orbital (HOMO), the lowest unoccupied molecular orbital (LUMO) and the energy gap between LUMO and HOMO plays a major role in governing many chemical reactions [21]. The energy of the HOMO is directly related to the ionization potential, and characterizes the susceptibility of the molecule toward attack by electrophiles, while the energy of the LUMO is directly related to the electron affinity, and characterizes the susceptibility of the molecule toward attack by nucleophiles. ΔE_g is an important stability index. A large ΔE_g value implies high stability for the molecule in the sense of its lower reactivity in chemical reactions [21, 25], i.e., a molecule with a smaller ΔE_g value is prone to forming a free radical. Thus, lnQ decreases with increasing ΔE_g.

The others three descriptors appearing the model of ln$Q$ are $\overline{q}_{MC^1,R^3}$, $\hat{q}_{AC^1,R^3}$ and R_{MC^1/R^3}. According to classical chemical theory, all chemical interactions are by nature either electrostatic (polar) or orbital (covalent). Indeed, it has been proven that local electron densities or charges are important in many chemical reactions and in determining the physicochemical properties of compounds [9]. Monomers, such as styrenes, with an unsaturated bond in R^3 easily form free radicals and possess larger ln$Q$ values; such monomers' APT charges on R^3 (q_{AR^3}) are obviously above the others. This phenomenon dictates that ln$Q$ is negatively correlated with $\hat{q}_{AC^1,R^3}$. Similarly, ln$Q$ is positively correlated with $\overline{q}_{MC^1,R^3}$, and negatively correlated with R_{MC^1/R^3}.

The optimum model of e consists of five descriptors (E_{LUMO}, q_{MC^1}, q^-, R_{MR^3/AC^1} and $R_{E_{LUMO}/\alpha}$) (see Table 3). It has been shown that a small energy gap between LUMO and HOMO (ΔE_g) usually means that the molecule is easily polarized [21], and the polarity of a molecule increases with decreasing E_{LUMO}, i.e., the parameter e is negatively correlated with E_{LUMO}. Since both E_{LUMO} and the average polarizability of molecules (α) correlate with e, the ratio of E_{LUMO} and α ($R_{E_{LUMO}/\alpha}$) also correlates with e. Furthermore, q^- correlates with e, which is easy to explain because atomic charges are also used to describe the molecular polarity and static chemical reactivity indices of molecules [9]. An attractive group in R^3 can result in a more positive Mulliken charge of C^1 (q_{MC^1}), which leads to the greater polarity of vinyl monomers and higher parameter e values. Thus q_{MC^1} correlates with e. The ratio of Mulliken charges on R^3 and APT charges on C^1 (R_{MR^3/AC^1}) correlates with e. The reason may be that the descriptor R_{MR^3/AC^1} can affect the parameter e, as does the descriptor q_{MC^1} .

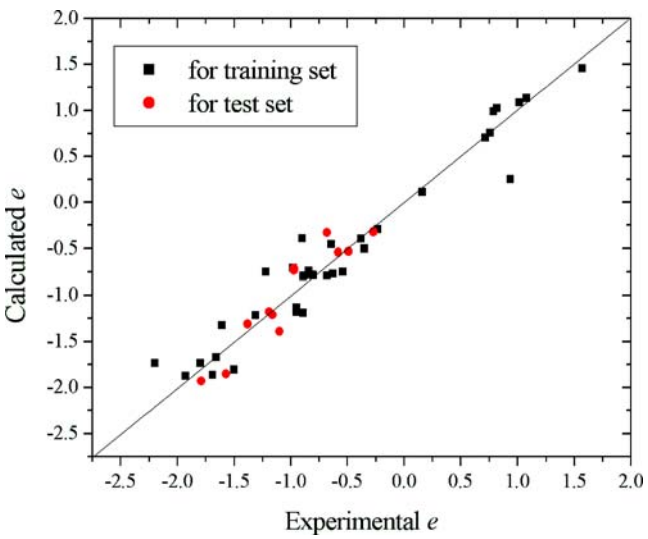

Fig. 2 Plot of calculated versus experimental e values

Conclusions

The reactivity parameters Q and e values of vinyl monomers in radical copolymerizations were predicted using QSPR models constructed by BP neural networks. The results indicate that the atom charges and FMO energies are the variables most correlatee with reactivity parameters of monomers (Q, e). The ANN modesl produced were proved to be accurate, with prediction set *rms* errors of 0.367 for ln$Q$ and 0.192 for e. These results encourage the further application of the proposed AAN models to other classes of monomers.

Acknowledgments The project was supported by the Scientific Research Fund of Hunan Provincial Education Department (NO. 07C205), and the Scientific Research Fund of Hunan Institute of Engineering (NO. 0761).

References

1. Alfrey T, Price CC (1947) J Polym Sci 2:101–109
2. Laurier GC, O'Driscoll KF, Reilly PM (1985) J Polym Sci: Polym Symp 72:17–26
3. Rogers SC, Mackrodt WC, Davis TP (1994) Polymer 35:1258–1267
4. Zhan CG, Dixon DA (2002) J Phys Chem A 106:10311–10325
5. Pan ZR (2002) Polymer Chemistry, 3rd edn. Chemical Industry, Beijing, pp 95–96
6. Semchikov YuD (1990) Vysokomolek Soedin A 32:243–252
7. Greenly RL (1980) J Macromol Sci Chem 4:427–443
8. Toropov AA, Kudyshkin VO, Voropaeva NL, Ruban IN, Rashidova SSh (2004) J Struct Chem 45:945–950
9. Karelson M, Lobanov VS, Katritzky AR (1996) Chem Rev 96:1027–1043
10. Yu XL, Xie ZM, Yi B, Wang XY, Liu F (2007) Eur Polym J 43:818–823
11. Yu XL, Yi B, Wang XY (2007) J Comput Chem 28:2336–2341
12. Brandrup J, Immergut EH, Grulke EA (1999) Polymer handbook, 4th edn. Wiley, New York
13. Parr RG, Yang W (1989) Density-functional theory of atoms and molecules. Oxford University Press, Oxford
14. Hobza P, Sÿponer J (1999) Chem Rev 99:3247–3276
15. Frisch MJ, Trucks GW, Schlegel HB, Scuseria GE, Robb MA, Cheeseman JR, Zakrzewski VG, MonTgomery JA Jr, Stratmann RE, Burant JC, Dapprich S, Millam JM, Daniels AD, Kudin KN, Strain MC, Farkas O, Tomasi J, Barone V, Cossi M, Cammi R, Mennucci B, Pomelli C, Adamo C, Clifford S, Ochterski J, Petersson GA, Ayala PY, Cui Q, Morokuma K, Malick DK, Rabuck AD, Raghavachari K, Foresman JB, Cioslowski J, Ortiz JV, Stefanov BB, Liu G, Liashenko A, Piskorz P, Komaromi I, Gomperts R, Martin RL, Fox DJ, Keith T, Al-Laham MA, Peng CY, Nanayakkara A, Gonzalez C, Challacombe M, Gill PMW, Johnson BG, Chen W, Wong MW, Andres JL, Head-Gordon M, Replogle ES, Pople JA (2003) Gaussian 03, Revision B.05. Gaussian, Pittsburgh, PA
16. Becke AD (1993) J Chem Phys 98:5648–5652
17. Hehre WJ, Radom L, Schleyer PvR, Pople JA (1986) Ab initio molecular orbital theory. Wiley, New York
18. Cioslowski J (1989) J Am Chem Soc 111:8333–8336
19. Fukui K (1975) Theory of orientation and stereoselection. Springer, New York, pp 34–39
20. Franke R (1984) Theoretical drug design methods. Elsevier, Amsterdam, pp 115–123
21. Zhou Z, Parr RG (1990) J Am Chem Soc 112:5720–5729
22. Mattioni BE, Jurs PC (2002) J Chem Inf Comput Sci 42:232–240
23. Gao JW, Wang XY, Li XB, Yu XL, Wang HL (2006) J Mol Model 12:513–520
24. Gao JW, Wang XY, Yu XL, Li XB, Wang HL (2006) J Mol Model 12:521–527
25. Lewis DFV, Ioannides C, Parke DV (1994) Xenobiotica 24:401–408